

Exploring the role of ammonia transporters (AMTs) in the branchial tissue of the horseshoe crab,
Limulus polyphemus

A thesis submitted to the Department of Biological Sciences, University of Manitoba in partial
fulfillment of the requirements for the course BIOL 4100 (Honours Thesis)

Bachelor of Science (Honours)

May 2023

Abstract

All organisms must manage ammonia as it is highly toxic and a product of many essential biochemical processes. One group of proteins that facilitates the movement of ammonia across cell membranes is the Ammonia Transport Protein family which are generally sorted into three groups—ammonia transporters (AMTs), Rhesus glycoproteins (Rh proteins), and methylamine permeases (MEPs)—expressed in plants, animals, and fungi, respectively. Recently, transcripts of AMTs have also been found in invertebrates, where experimental evidence suggest that they play a role in both ammonia excretion and ammonia sensing. The American horseshoe crab, *Limulus polyphemus*, expresses at least two AMT and two Rh proteins within the epithelia of their book gills which is the primary surface for ammonia excretion. Each gill lamellae have a ventral ammonia permeable side and a dorsal ammonia impermeable side. mRNA transcripts for both proteins LpAMT-1 and LpAMT-3 were found on the dorsal and ventral surfaces, bringing into question their function in direct ammonia excretion. In oocyte expression trials both AMTs failed to mediate the transport of radiolabeled methylamine, while transport was detected for both a coral and a human Rh protein. Direct evidence of ammonia transport by invertebrate AMTs has not been previously found and further research should be conducted into the function of these proteins in invertebrates.

Special Acknowledgements

I would like to extend my sincerest thanks to the students and faculty that made this project possible. I would like to thank my supervisor Dr. Dirk Weihrauch for his continuous advisement and support throughout the project and for always having his office open to me and his other students. I would like to extend my gratitude to the other members of my committee, Dr Kevin Campbell and Dr Jason Treberg for their input and for their assistance in developing the project and improving my skills as a scientist. I would like to thank the other members of Dr Weihrauch's lab. In particular, Dr Alex Quijada-Rodriguez for contributing his time to both the lab work and theoretical discussion necessary to complete this project. An additional thanks to Ruotong Liu for her time and experience in the injection and incubation of the *Xenopus* oocytes, without her microinjection skill and guidance this project would have been beyond the scope of an undergraduate student. I am deeply grateful for all involved in the creation of this project including all who have discussed it with me in a less official capacity. I know that I shall look back on this term as a formative step in my journey as a scientist and that is due to the unwavering support of my peers in the Faculty of Biological Sciences.

Table of Contents

Abstract	i
Special Acknowledgements	ii
List of Tables	iv
List of Figures	v
Introduction	1
<i>Other possible functions</i>	4
<i>Limulus polyphemus</i>	7
<i>Objectives</i>	9
Methods	10
<i>Animal handling and lamellae sectioning for tissue sampling</i>	10
<i>RNA isolation and PCR</i>	11
<i>Functional expression analysis of LpAMT1 and LpAMT3</i>	14
<i>Day 0: Oocyte harvest</i>	15
<i>Day 1: Injection and incubation</i>	16
<i>Day 4: Exposure</i>	16
<i>Statistical analysis</i>	17
Results	18
<i>Sequence analysis of LpAMT1 and LpAMT3</i>	18
<i>Functional expression of LpAMT1 and LpAMT3</i>	22
Discussion	25
<i>Protein alignment</i>	25
<i>PCR localization</i>	25
<i>Oocyte expression</i>	26
<i>Conclusion</i>	29
Literature	30

List of Tables

Table 1: Primer sequences used in PCR with their associated Genbank accession number, amplicon size and annealing temperature	14
---	----

List of Figures

Figure 1: Diagram of ventral *L. polyphemus* anatomy indicating three main body regions, the prosoma, the opisthosoma and the telson. Arrow indicates the opisthosomal flaps that cover the book gills, within the blue box is one extracted lamellae, ventral side up with the outer edge to the left side. A) Central mitochondrial-rich area (CMRA); (B), peripheral mitochondria-poor area (PMPA); (C), branchial setae; (D), hardened outer edge of the lamellae, appropriate for handling. 8

Figure 2: Alignments of known AMT amino acid sequences with highly conserved regions important for ammonia transport function are highlighted in yellow (Javelle et al. 2006; Andrade and Einsle 2007). Regions highlighted in green are relevant for the electrogenic function of AtAMT1;2. (Neuhäuser and Ludwig 2014) The sequence in gray is the carboxyterminal region that is highly conserved in Arabidopsis and other plant AMTs and is implicated in monomer-monomer interactions (Neuhäuser et al. 2007). 19

Figure 3 Qualitative PCR results across the four tissue sections. Dorsal half lamellae, peripheral mitochondria poor area, central mitochondrial rich area, branchial setae. Transcripts and predicted amplicon sizes: elongation factor 1- α (122 bp), LpAMT-1 (149bp) LpAMT-3 (213bp) LpRh-1 (173bp), LpRh-2 (190bp) Visualized on 1% Agarose gel with ethium bromide..... 21

Figure 4: Radiolabelled methylamine uptake in picomole of methylamine per oocyte per hour ($\text{pmol}^{-1}\text{oocyte}^{-1}\text{hour}$) from oocytes injected with the 18ng cRNA coding for protein LpAMT-1 (4A green, n=28), LpAMT-3 (4A yellow, n=28), AyRhp-1 (4B red, n=25), human Rh (4B purple, n=27) molecular grade water (sham, blue, n=28). Exposure to 1mM methylamine for 60 minutes with 1 uL of C14 labelled MA (define this acronym) per 500uL. Counts taken for five minutes per oocyte and divided by five to find the average count per minute. * Indicates a mean significantly different than that of sham in an unpaired T= test ($p<0.05$). 23

Figure 5: Radiolabelled methylamine uptake in counts per minute per oocyte (CPM) with competitive inhibition. Exposure to 1mM methylamine for non inhibition trials and 1mM methylamine + 1mM ammonium chloride (+ NH_4^+) for inhibition trials. Exposure for 60 minutes with 1 uL of C14 labelled MA per 500uL of incubation buffer. Counts taken for five minutes per oocyte and divided by five to find the average count per minute. Oocytes injected with the 18ng cRNA coding for proteins LpAMT-1 (green, n=28 non inhibition, n=27 inhibition), LpAMT-3 (yellow, n=28 non inhibition, n=28 inhibition) or molecular grade water (sham, blue, n=28 non inhibition, n=26 inhibition). * Indicates a mean significantly different between the non inhibition and inhibition groups of the same cRNA insert ($p<0.05$)..... 24

Introduction

Along with carbon, oxygen, and hydrogen, nitrogen is among the most common essential elements that are needed for an organism to live and grow. Nitrogen is a building block for nucleic acids, amino acids, and other essential biological molecules. The simplest form of nitrogen that can be used by most organisms is ammonia. Ammonia is the preferred form of nitrogen taken up by most plants and can be used directly in the formation of other nitrogenous molecules (Howitt and Udvardi 2000). Ammonia is also produced by around 200 different enzyme reactions and is considered an essential metabolite (Molnár and Fekete 2011). Despite its importance, ammonia is also extremely toxic at higher concentrations: it is disruptive to intercellular and extracellular pH and competes with important ions in ion exchange mechanisms, leading to impeded nerve signaling and causing cellular dysfunction. (Binstock and Lecar 1969; Larsen et al. 2014). Given both its importance in forming molecules and its toxicity it is necessary that all organisms have control over the movement of ammonia across cell membranes and within tissues. Originally it was thought that the movement of ammonia occurred purely through diffusion as NH_3 across cell membranes. However, ammonia is amphoteric and exists in two forms in aqueous solution, the ionic form, NH_4^+ , and the gaseous, uncharged form, NH_3 . While NH_3 can diffuse across cell membranes with relative ease, NH_4^+ , like other ions, needs some form of facilitated transport system to allow it to enter or exit cells. With a pKa of ca. 9.25, $\text{NH}_4^+/\text{NH}_3$ exists overwhelmingly in the ionic form at physiological pH levels and hence needs an effective mode of transportation to exit cells (Wright 1995).

One common ammonia transport system across nearly all lineages, both prokaryotic and eukaryotic, are membrane bound proteins in the ammonium transporter/methylammonium

permease/Rhesus protein family (AMT/MEP/Rh family) that allow for the movement of ammonia (NH_3) or ammonium ions (NH_4^+) across cell membranes (McDonald and Ward 2016). Conventionally, the family is divided into three definite clades, AMTs in plants, MEPs in fungi, and Rh proteins in animals. AMT proteins are considered to be the most ancestral, as they are present in all kingdoms of life. Vertebrates however, have lost the ancestral orthologs of AMT proteins and are thought to only have the more derived Rhesus type proteins (Peng and Huang 2006). This has led to Rh proteins being considered the animal equivalent to the primitive plant AMT proteins. Despite this, co-occurrence of genes from both clades is common in microbes and invertebrate animals (Huang and Peng 2005; McDonald and Ward 2016). The potential roles and functions of plant-like AMTs in animals have only been partially explored.

Research is still ongoing about the differences in function and structure between Rh and AMT proteins. There are multiple highly conserved regions present across both groups that are essential for the transport function. Ammonia transport proteins are trimeric, being formed of three monomers. Each monomer has 11 or 12 transmembrane regions that form an open pore. Transport of ammonia occurs through the pore in the center of each monomer. There are multiple suggested modes of transporting ammonia but many AMTs found in plants are electrogenic (i.e. moving a positive charge across the membrane), meaning they either transport the ammonium cation or cotransport ammonia gas and a proton (Andrade and Einsle 2007).

The electrogenic transport of NH_4^+ by AMT proteins is accomplished by the structural properties of a number of highly conserved regions. On the extracellular side of each monomer there is an ion specific binding site responsible for the recruitment of NH_4^+ that is thought to be involved in the channel's high substrate affinity. Other highly conserved regions include a phenylalanine gate that occludes the pore while the substrate passes through and a twin pair of

histidine residues on the inside of the pore, with both of these features contributing to the transport functions of AMT proteins (Javelle et al. 2006). Briefly, these highly conserved structures are thought to cause the deprotonation of NH_4^+ into NH_3 outside of the cell, allowing NH_3 to diffuse through the pore guided by the pair of histidine residues that lie within the pore. This conformation allows for high ammonia affinity in plants and fungi, facilitating efficient ammonia uptake even if concentrations are low (Ninnemann et al. 1994). The pathway for the dissociated proton is less clear but it has been found that altering the charge of amino acids in the subunit contact sites within the trimer of *Arabidopsis* AMT AtAMT1;2, reduced NH_4^+ dependent ionic currents while maintaining detectable NH_3 transport. This suggests that the proton passes between the monomers as opposed to through them alongside the deprotonated NH_3 molecule (Neuhäuser and Ludewig 2014).

In animals, who do not get their nitrogen directly from the environment but rather from the nitrogenous compounds of the foods they eat, the assimilation of nitrogen from the environment is not the suggested function of these AMT proteins. As ammonia is a common nitrogenous waste product in animals their proposed function is excretion (Durant and Donini 2018). As ammonia is water soluble, aquatic species have abundant water available to dilute this toxic substance in their body fluids. With few exceptions such as elasmobranchs and adult amphibians, aquatic animals are generally ammoniotelic, releasing ammonia directly into the water (Larsen et al., 2014, Wright, 1995). Consequently, with this lifestyle their demand for an efficient ammonia excretion mechanism is quite high. It is common for marine invertebrate species to have multiple different transport proteins from both the Rh and AMT clades that may be contributing to the excretion of ammonia. The marine polychaete, *Eurythoe complanata*, has one Rh protein and three AMT proteins in its branchial tissue that, along with Na^+/K^+ -ATPase

(NKA), V-type H⁺-ATPase (HAT) and carbonic anhydrase (CA), are implicated in the excretion of ammonia (Thiel et al. 2017). This study confirmed that the three AMTs are expressed in the same tissue from which ammonia is being excreted. Their involvement in invertebrate ammonia excretion was also suggested due to the upregulation of mRNA expression in mosquito larvae when exposed to high environmental ammonia conditions (Durant and Donini 2018). However, no functional expression or direct measure of AMTs moving ammonia was performed. Other evidence for the excretory capabilities of invertebrate AMTs includes a study where the authors showed that *Aedes aegypti* larva with its AMT expression in the excretory anal papillae knocked down, had a 60% decrease in ammonia excretion across their excretory anal papillae (Chasiotis et al. 2016).

Interestingly, while the ammonia transport capabilities of invertebrate Rh proteins has been demonstrated, e.g. in a yeast complementation assay in *C. elegans* (Adlimoghaddam et al. 2015), no evidence has been provided so far that AMTs expressed in animals are directly transporting ammonia.

Other possible functions

The most ancestral AMT/MEP proteins were likely used in the direct assimilation of ammonia in the same way they are currently being used by single-celled organisms, e.g. bacteria and yeast, and plants. The importance of these proteins in the assimilation of ammonia can be illustrated by the inability of yeast MEP knockdown mutants to thrive on media that contains ammonia as the sole nitrogen source (Marini et al. 2000). Along with this assimilation function, there is evidence of both fungal MEPs and bacterial AMTs having a sensory function. It has been suggested that these proteins induce or suppress multiple regulatory pathways that confer organism wide ammonia response (Tremblay and Hallenbeck 2009). These responses include the

initiation of the pseudohyphal growth states in fungi. In wild type *S. cerevisiae*, there is a transition from a round growth form into a filamentous growth form when they are starved for ammonia or other nitrogen sources. The protein MEP-2 is essential for the initiation of filamentous growth in situations where the change in growth pattern would normally occur. This indicates that in *S. cerevisiae* MEP-2 is not only transporting ammonia but responsible for delivering signals about environmental ammonia to the cell (Lorenz and Heitman 1998). Similar results were found for the yeast *Candida albicans*, where loss of function mutants were unable to transition between growing states (Biswas and Morschhäuser 2005).

Terrestrial invertebrates also have both AMT and Rh proteins; however, as they are not submerged in water the excretion of ammonia directly into the environment is not possible, bar a handful of exceptions e.g. terrestrial crustaceans like *Porcellio scaber* and small terrestrial isopods who excrete ammonia by volatilization into the air. (Wright et al. 1994). Most terrestrial animals use alternative types of nitrogenous waste, primarily uric acid or urea (Wright 1995). Accordingly, they would not have the same need for ammonia excretion as an ammoniotelic species. Terrestrial invertebrates still retain AMT-type proteins, even those that are not known to excrete ammonia; therefore, the transporters must have an alternate function. AMTs of insects have been implicated in sensory functions (Vulpe et al. 2021). AMT proteins in the antennae of both flies and mosquitos are known to form a non-canonical sensory pathway for the detection of ammonia. In *Drosophila melanogaster* it was found that, upon the elimination of canonical olfactory pathways from sensory hairs upon their antennae, the presence of AMT proteins was enough to trigger an ammonia response. The elimination of these proteins in *D. melanogaster* resulted in an inability to detect ammonia. This ability could be restored by introducing an AMT from either *D. melanogaster* or *Anopheles gambiae* (Vulpe et al. 2021). These data would

indicate that the sensory function of AMT is conserved across insect families. In adult female *A. gambiae* mosquitos, both AMT and Rh proteins were highly expressed in the antennae and shown to be electrogenic. Briefly, voltage changes on either side of the cell membrane of a *X. laevis* oocytes expressing the mosquito AgAMT protein when exposed to ammonia in solution (Pitts et al. 2014). However, AgAMT transformation failed to complement MEP deficient yeast strains in this same study, showing no evidence of nitrogen transport for AgAMT.

When considering a model organism to explore the function of invertebrate AMTs there are many factors to consider. The American horseshoe crab *Limulus polyphemus* has many favorable traits to study ammonia transport proteins. They are known to be ammoniotelic and to transport ammonia across their book gill epithelia (Hans et al. 2018). Their genome and transcriptome have both been sequenced and published. Several transcripts for proteins involved in ammonia excretion, including two Rh proteins (LpRh-1 and LpRh-2), Na⁺/K⁺-ATPase (NKA), and hyperpolarization-activated cyclic nucleotide gated K⁺ channel (HCN) have been located within the gill lamellae. In addition, *L. polyphemus* is the last extant species of its genus and one of only four extant species in the order *Xiphosura* (Lamsdell 2020). Most species within *Xiphosura*'s closest related taxa are non-ammoniotelic terrestrial arachnids such as spiders and ticks though whether the placement of this clade is within or alongside class *Arachnida* is still contested (Ballesteros and Sharma 2019). This makes *L. polyphemus* a species of particular interest to evolutionary biologists, particularly when investigating the evolution of different modes of nitrogen excretion.

Limulus polyphemus

L. polyphemus carries five pairs of book gills along the ventral surface of the opisthosoma with each book gill having over 100 lamellae. Each lamella is divided into four regions of distinct composition. The lamella is composed of two half lamellae, the dorsal lamella, and the ventral lamella. The ventral lamellae are ion permeable ($G_{te} = 145 \text{ mS cm}^{-2}$) and the main site of ammonia excretion (Hans et al. 2018). The dorsal lamellae are rather ion impermeable ($G_{te} = 0.2 \text{ mS cm}^{-2}$) which is believed to act as a protective barrier against passive reabsorption of excreted waste when stacked on top of each other in the book gill conformation. Under physiological conditions the dorsal lamella promotes no ammonia transport (Hans et al. 2018). The ventral half lamella is composed of two regions, the central mitochondria-rich area (CMRA; Fig.1A) and a peripheral mitochondria-poor area (PMPA; Fig 1B) that have differences in transport protein expression with regards to the two different Rh proteins and NKA (Hans et al. 2018) though differences in excretion rates between the CMRA and PMPA have not been measured. In addition, on the outer rim of each gill lamella, marginal branchial setae can be seen, though their function has not yet been explored (Fig.1C).

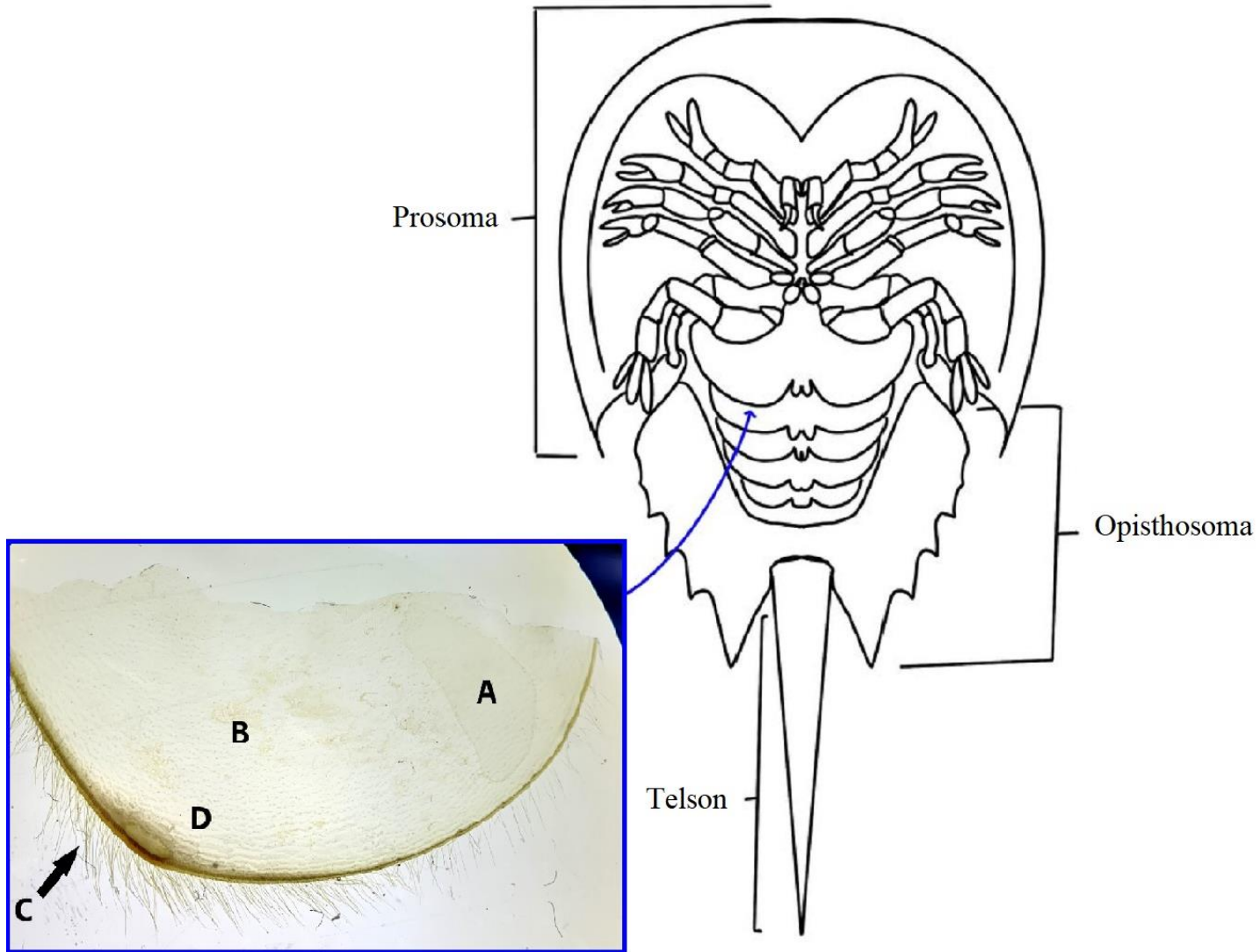


Figure 1: Diagram of ventral *L. polyphemus* anatomy indicating three main body regions, the prosoma, the opisthosoma and the telson. Arrow indicates the opisthosomal flaps that cover the book gills, within the blue box is one extracted lamella, ventral side up with the outer edge to the left side. A) central mitochondrial-rich area (CMRA); (B), peripheral mitochondria-poor area (PMPA); (C), branchial setae; (D), hardened outer edge of the lamella, appropriate for handling.

Objectives

Two different AMTs (LpAMT-1 and LpAMT-3) have been found by PCR in the branchial tissues of *L. polyphemus*. Previous studies have also found differences in both protein expression and ammonia permeability across different regions of the gill (Hans et al. 2018). However, it is currently unknown in which of the gill sections LpAMT-1 and LpAMT-3 are found. Based on the differing ammonia transport capabilities of the dorsal and ventral lamellae, I hypothesized that LpAMT-1 and LpAMT-3 are present in the ammonia transporting ventral lamellae. No prediction can be made about which region of the ventral lamella they would be located in (CMRA or PMPA) due to previous ammonia excretion studies not differentiating between the two regions. For the purposes of the experiment the null hypothesis would be that they are uniformly distributed across the two regions.

Up until this point the branchial setae on the lamellar margins have not been characterized. It was previously shown that AMTs are found in the antennae of mosquitoes and were involved in the detection of ammonia. Thus, it is possible that LpAMT-1 and LpAMT-3 found in the branchial setae also have a potential sensory function.

There is currently no direct experimental evidence that AMT proteins in invertebrates are transporting ammonia. The literature offers some indirect evidence of ammonia transport, as ammonia transport rates are reduced in larval mosquito *Aedes aegypti* when their AMT expression is knocked down (Durant and Donini 2018). An increase in current was also found when the antennal expressed *Anopheles gambiae* protein AgAMT was expressed in oocyte expression experiments, though the accompanying yeast complementation assay to demonstrate nitrogen movement showed no ammonia assimilation (Pitts et al. 2014). Functional expression

experiments should provide valuable insight into the function of these proteins, whether they are transporting ammonia or not.

Methods

Animal handling and lamellae sectioning for tissue sampling

Eight adult horseshoe crabs were obtained for this study and were kept in the Animal Holding Facility (University of Manitoba, Winnipeg, Manitoba, Canada) in tanks of aerated and filtered artificial seawater at 32-33 ppt salinity at a temperature of 20°C. The crabs were held in groups of two to four individuals depending on size but their enclosures were part of the same circulating artificial seawater system to minimize differences in water composition between tanks. Crabs were kept on 2-4 cm of aragonite sand substrate that allows for natural burrowing behaviors, and fed a diet of raw mussels, raw shrimp, and raw scallops twice a week (Monday and Friday).

Prior to removing the gill lamellae, animals were cooled by being placed on ice for 20-45 minutes and monitored as the speed of cooling was variable and loosely based on the size of the individual. Once the movement and reflex time slowed, indicating that they were cooled enough for handling with limited risk to handler or animal, tissue sampling was initiated. Removal and sectioning of 8 to 10 lamellae from each animal was done as quickly as possible to reduce handling time of the animal and to minimize the degradation of the mRNA.

Removal of the lamellae was done with tweezers and a pair of sharp, RNase-free micro-scissors. The side that the lamellae were taken from was noted before tissue sectioning so that as the tissue was sectioned, dorso-ventral orientation was not lost. Only lamellae that were free of obvious pathologies including parasitic infection or previous tissue damage were collected and

any pathology or damage on adjacent lamellae was noted as a potential variable in downstream analyses.

Once removed, lamellae were sectioned into their four gill regions under a dissecting microscope. Fine tweezers were used to grab the hardened outer rim (Figure 1D) and a sterile 25-gauge hypodermic needle was inserted along the cut edge and used to separate the dorsal half from the ventral half. The needle was exchanged between crabs but not between individual lamellae. The ventral half was further sectioned into the CMRA (Figure 1A) and PMPA (Figure 1B). In preliminary RNA purifications there was consistently higher mRNA yield from isolations of the CMRA tissues per weight when compared with the PMPA, which resulted in the decision to leave slim margins around the CMRA when tissue sectioning. This would mean that contamination of the CMRA with PMPA mRNA is more likely than the contamination of the PMPA with CMRA RNA, as CMRA tissue would likely have had the greater effect on the PCR result. The final step was the removal of the branchial setae from the marginal edge using a scalpel. As RNA was not isolated immediately each tissue section was submerged in 700 μ L of *RNAlater* Stabilization Solution (Fisher Scientific) and stored for at least three hours at room temperature to allow the solution to permeate the tissues before being placed into the fridge (4°C) where the samples were stored overnight. After that the samples were moved to a -20°C freezer.

RNA isolation and PCR

The isolation of mRNA from the sectioned gill lamellae were performed using the Monarch[®] Total RNA Miniprep Kit following the manufacturer's instructions (New England Biolabs). Once the tissue samples had been removed from cold storage, they were removed from *RNAlater* storage solution and blotted dry on a fresh Kimtech Science[™] wipe before being transferred into 600 μ L of 1x DNA/RNA protection reagent. This reagent was diluted from the

2x solution provided in the kit by adding equal volume of molecular grade water just before isolation. Tissue and reagent were combined in a manual glass homogenizer. Both dorsal and PMPA tissue samples were divided roughly in two and only half the sample used in the extraction due to the predictably higher volume of both tissues compared to the CMRA and branchial setae within the lamella. The glass homogenizers fit snugly into their tubes and acted as a mortar and pestle with a high contact surface between the tool and the sample resulting in adequate homogenization. The final RNA concentration was determined on a spectrophotometer (Nanodrop, ND-1000, Thermofisher, Waltham, MA, USA).

Before reverse transcription the purity of the RNA and the effectiveness of the DNase I treatment step was evaluated by PCR using EconoTaq[®] PLUS GREEN 2x Master Mix Primer pairs for elongation-factor-1-alpha (Lp-EF1 α , Table 1) to check for genomic DNA. As this check resulted in a faintly positive result (data not shown), a second DNase I treatment (ThermoScientific) was done to improve the confidence of any conclusions drawn from my reverse transcribed mRNA results. This entailed adding 1 μ L of 10x DNase reaction buffer and 1 μ L of DNase 1 to 8 μ L of RNA. RNA samples of all tissue types for a single crab were diluted to match the RNA sample of the lowest concentration, ensuring that each tube within a tissue set had the same amount of RNA within the 8 μ L added to the DNase 1 reaction. This lowest concentration was universally from the branchial setae as they had the smallest mass of starting material. The DNase 1 reaction was incubated at 37°C for thirty minutes before 1 μ L EDTA was added per tube, and it was further incubated for 10 minutes at 65°C to inactivate the enzyme. After the reaction 1 μ L of each tube was re-evaluated by PCR with the Lp-EF1 α primer pair (see Table 1) and produced no PCR product (data not shown).

The purified mRNA was then reverse transcribed into cDNA using the LunaScript[®] RT SuperMix Kit (New England Biolabs, MA, USA). Each 20 μ L reverse transcriptase (RT) reaction contained 10 μ L DNase treated mRNA, 4 μ L of LunaScript mix and 6 μ L molecular grade water. The reaction was held at 25°C for two minutes for initial denaturation, then at 55°C for ten minutes for reverse transcription. The final step was one minute at 95°C to denature the enzyme. The reverse transcribed cDNA was then diluted to 40 μ L and placed in -20°C storage between PCR reactions.

Once there was a complete set of RT cDNA from all four tissue sections of the same crab they were tested using qualitative PCR for the presence or absence of LpAMT-1, LpAMT-3, LpRh-1 and LpRh-2. The PCR thermocycle protocol consisted of an initial denaturation temperature of 98°C for two minutes followed by 35 cycles of 94°C for 20 seconds, the primer pairs preferred annealing temperature (Table 1) for 20 seconds, and an elongation step at 72°C for 40 seconds. Final elongation was held at 72°C for three minutes before holding at 20°C indefinitely. Tubes were prepared on ice and moved to the thermocycler after it had reached initial denaturation temperature. PCR amplification results were visualized on a 1% agarose gel with 1 μ L ethidium bromide added per 25 mL gel. As the PCR was qualitative, the target mRNA sequence was considered present in the tissue section if there was any visible band of appropriate amplicon size regardless of intensity.

Table 1: Primer sequences used in PCR with their associated Genbank accession number, expected amplicon size and annealing temperature

Transcript	GenBank accession #	Forward primer	Reverse primer	Amplicon size bp	Annealing temp °C
EF-1 α	XM_013928278.1	GGCTACAATCCTGCCACTGT	GTTTGACCCTTGCGTTCAAT	122	58
LpAMT-1	XM_022393282.1	CGGGGTTGGTTCATATTTTG	TGCAGTAAGCCACGAAACTG	149	50
LpAMT-3	XM_022382768.1	CCTGGAACATTGCAGGAA	GGTTGCCATCTTGTGCAT	213	50
LpRh-1	XM_013920039.1	TGGTTTCATCTCGGTTATGGG	AGCTGTAACCGTAGTTGTCTTC	173	58
LpRh-2	XM_013917394.1	CCCTGTTCAATTGGTTGTGATG	GGTCTTTAGAGGGATCCTGAAG	190	58

Functional expression analysis of LpAMT1 and LpAMT3

Xenopus laevis oocytes have been one of the most common systems in which to observe the function of ion channels and neural receptors (Goldin 1993). Oocytes have stores of all the enzymes and proteins necessary in the early development of *X. laevis* embryos after fertilization. In the absence of fertilization, foreign sequences (mRNA or cDNA) may be added to the cytoplasm and take advantage of the cells' protein manufacturing systems to express large quantities of the added protein (Miller and Zhou 2000). This system has the advantage of being able to synthesize one or more proteins from exogenous mRNA sequences, allowing them to be studied in relative isolation (Goldin 1993). The microinjection of LpAMT-1 and LpAMT-3 mRNA should result in a system where their potential ammonia transport function can be observed.

The open reading frames for each AMT were taken from the transcriptome and extended with the addition of the restriction sites SmaI (5' end) and XbaI (3' end). The extended open reading frames were then ligated into the expression vector pGEM®-HE using a T4 ligase, and the plasmids transformed into DH5- α *Escherichia coli* competent cells (Thermo Fisher Scientific™, MA, USA). Each insert was amplified, extracted, and had its sequence verified. The vector was then linearized and transcribed into capped mRNA (cRNA) using the mMACHINE™ T7 Transcription Kit (Thermo Fisher Scientific Inc., Waltham, MA, USA) for injections into the *X. laevis* oocytes.

Day 0: Oocyte harvest

With the assistance of veterinary services, one gravid female *Xenopus laevis* was anesthetized in tricaine methane sulfonate (MS-222), the frog was humanely euthanized via decapitation and its ovary removed. The removed ovary was rinsed in standard calcium-free oocyte ringer (OR2: 82.47 mmol/L NaCl; 5.45 mmol/L HEPES; 2.5 mmol/L KCl; 1 mmol/L MgCl₂; 1 mmol/L Na₂HPO₄; pH=7.6) until the blood was washed away. The ovary was then placed in fresh calcium-free OR2 buffer along with 0.5 mg/L collagenase type IV and gently agitated to facilitate digestion and the separation of the oocytes from the ovary membrane. After a period of 3-4 hours, the connective tissue was digested, to the point that oocytes flowed freely through the media when agitated. The loose oocytes were then washed with standard oocyte ringer (OR2: 82.47 mmol/L NaCl; 5.45 mmol/L HEPES; 2.5 mmol/L KCl, 1 mmol/L MgCl₂; 1 mmol/L Na₂HPO₄; 1 mmol/L CaCl₂ pH=7.6). The added CaCl₂ in the buffer solution terminated the collagenase activity to avoid over digestion. Oocytes were sorted for the trials based on visual parameters, primarily uniformity and size. The chosen oocytes were placed in fresh OR2 that was supplemented with 0.5 mmol/L sodium pyruvate as an exogenous energy source, 10

mL/L penicillin-streptomycin, and 0.23 mmol/L gentamicin to avoid bacterial development outside the ovary. Oocytes were then left to incubate overnight at 18°C.

All procedures performed were approved by the University of Manitoba Animal Research Ethics committee in accordance with the Guidelines of the Canadian Council on Animal Care (Protocol #: F20-021/1).

Day 1: Injection and incubation

After overnight recovery, individual oocytes were injected with 18 ng of cRNA (36.8 nL/oocyte of 500 ng/μL) using a Nanoject III auto-nanoliter injector (Drummond Scientific, Broomall, PA, USA). There were five treatment groups, a sham injection of molecular grade water, cRNA of LpAMT-1, cRNA of LpAMT-3 and two positive controls, cRNA of a coral (*Acropora yongei*) Rh protein ayRhp1 (Thies et al. 2022) and cRNA from human Rh protein. The human RhCG protein was selected as a positive control due to it being the Rh protein with the most supporting literature. The coral Rh was chosen for its availability, high transport affinity and its similarity to invertebrate Rh protein transcripts (Thies et al. 2022). About 60 oocytes were injected per treatment group. These oocytes were returned to the incubator for three days to allow them to begin expressing the injected mRNA. Each day they were checked, dead oocytes were removed, and the surviving oocytes were transferred to fresh buffer before returning to the incubator.

Day 4: Exposure

On day four the oocytes were ready for the exposure and methylamine transport trials. Two buffers were made, the first being the OR2 buffer with the addition of 1 mmol/L methylamine, the second was the OR2 buffer with 1 mmol/L methylamine and 1 mmol/L of

ammonium chloride to measure competitive inhibition of methylamine transport. If the transporter was in fact transporting ammonia, there should be less methylamine uptake in those treated with the second buffer as it should be competing with the ammonia for transport. Just before the exposure, 1 μ L of C14 radiolabeled methylamine was added for every 499 μ L of buffer resulting in a buffer radioactivity counts of between 1700 and 2000 counts per minute (cpm) per microliter. Exposure treatments were done sequentially with each treatment beginning five minutes before the next treatment so that when they were removed 60 minutes later, they could be washed and have each oocyte isolated before the next group had to be pulled. The isolated oocytes were transferred into a 6 mL pony vial (Perkinelmer Inc.). 200 μ l of 10% sodium dodecyl sulfate (SDS) solution was added into each vial to dissolve the oocyte and release the contents. Finally, 2 mL of Ultima Gold liquid scintillation cocktail (Perkinelmer Inc.) was added to each vial. The internal radioactivity of each oocyte was counted with a Tri-Carb 3110TR Liquid Scintillation Analyzer (Perkinelmer Inc.) in counts per minute per oocyte to then be converted into in pmol per hour per oocyte . The cpm of each buffer was measured three times and by the scintillation analyser and the average of these values was used to calculate the uptake in pmol per hour per oocyte. This was done to account for small differences in average cpm between the incubation buffers. Each treatment was three groups of ten oocytes, or as close as could be achieved with the number of oocytes that survived per injection group.

Statistical analysis

All data is presented as a five number summary box and whisker plot (Figure 4, Figure 5). Each dataset's distribution was evaluated using a Shapiro-Wilk test to ensure that they were suitably normally distributed for other parametric tests. Grubbs tests were performed on the outputs of each treatment group to exclude outliers (for example, due to damage or injury to the

oocyte altering transport functions). Unpaired T-tests were run to compare to mean of the sham treatment group the mean of each of the other treatment groups. For evaluation of competitive inhibition each T-tests were run only between treatment groups and their associated competitive inhibition treatment group.

Results

Sequence analysis of LpAMT1 and LpAMT3

Using the program Clustal Omega, LpAMT-1 and LpAMT-3 primary structures were aligned with a selection of other protein sequences from the electrogenic AMT protein family (Figure 2). These included the *A. thaliana* protein AtAMT1;2 due to there being data regarding regions that are integral for both ammonia transport and electrogenic function of the protein (Neuhäuser et al. 2007; Neuhäuser and Ludwig 2014), and the *A. gambiae* protein AgAMT as an invertebrate AMT protein with established electrical function and sensory implications (Pitts et al. 2014). Both *L. polyphemus* AMT proteins LpAMT-1 and LpAMT-3 have the highly conserved regions that are known to be essential to transport function such as the phenylalanine gate and the two central histidines. They also have all 11 transmembrane regions that would be expected of a protein of this class. However all three invertebrate AMTs had insertions in the highly conserved C-terminal section that is integral to transport function in AtAMT1;2 and other plant proteins (Neuhäuser et al. 2007).

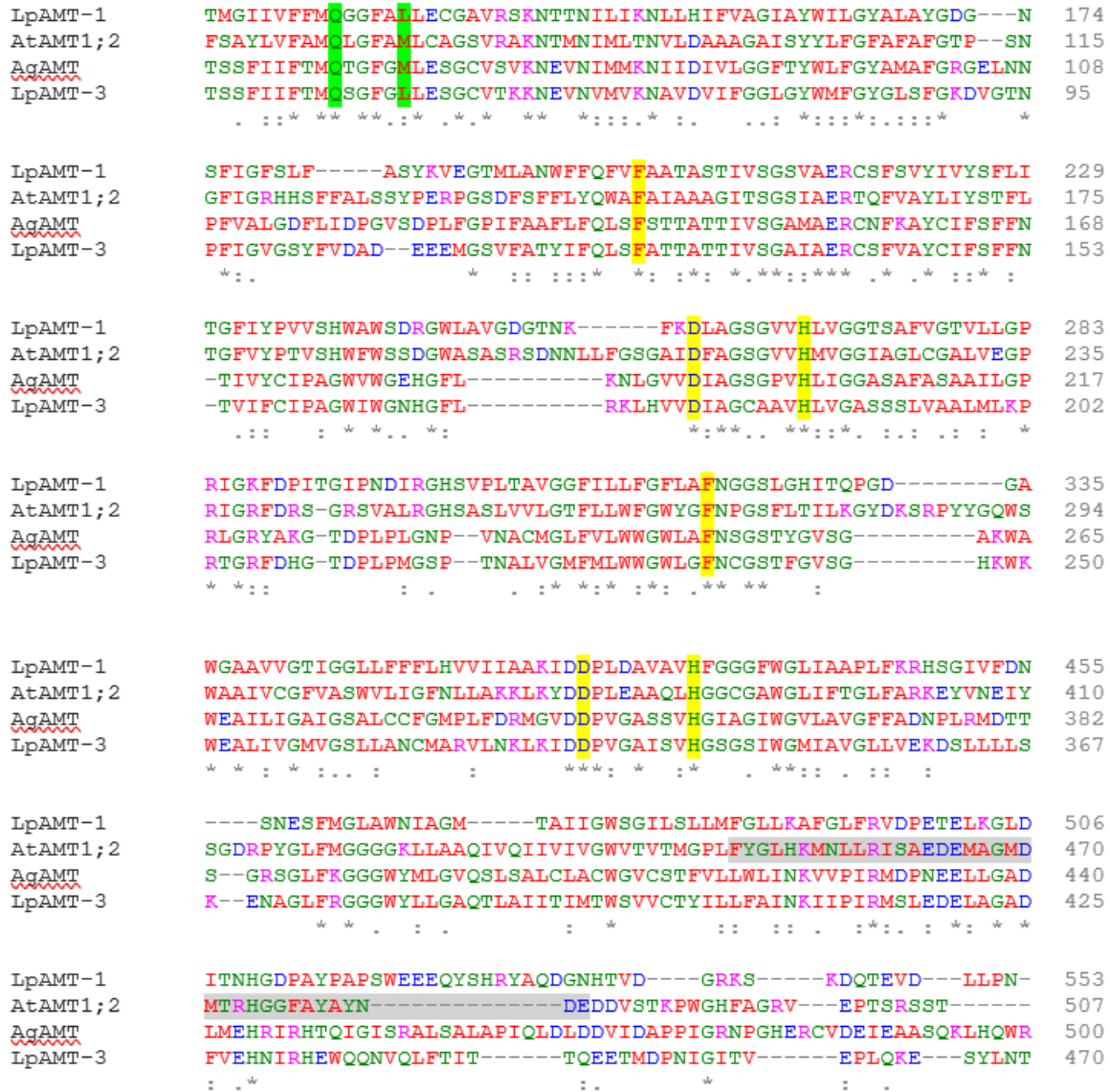


Figure 2: Alignments of representative AMT amino acid sequences with highly conserved residues important for ammonia transport function highlighted in yellow (Javelle et al. 2006; Andrade and Einsle 2007). Regions highlighted in green are relevant for the electrogenic function of AtAMT1;2. (Neuhäuser and Ludewig 2014). The sequence in gray is the carboxyterminal region that is highly conserved in *Arabidopsis* and other plant AMTs and is implicated in monomer-monomer interactions (Neuhäuser et al. 2007). Asterisks indicates positions which have a single, conserved residue. Colons denote conservation between residues with highly similar properties, Periods indicates conservation between groups with lightly similar properties. Text colours indicate different properties: red, small and hydrophobic; blue, acidic; magenta, basic; green, hydroxyl + sulfhydryl + amine.

Branchial expression of LpAMT1 and LpAMT3

In the qualitative PCR, EF1- α acted as positive control and therefore had the expected band across all tissue sections. For all other primer pairs there was at least a faint band across every tissue section though the intensity of the signals from the branchial seatae cDNA never matched the intensity of the positive controls.

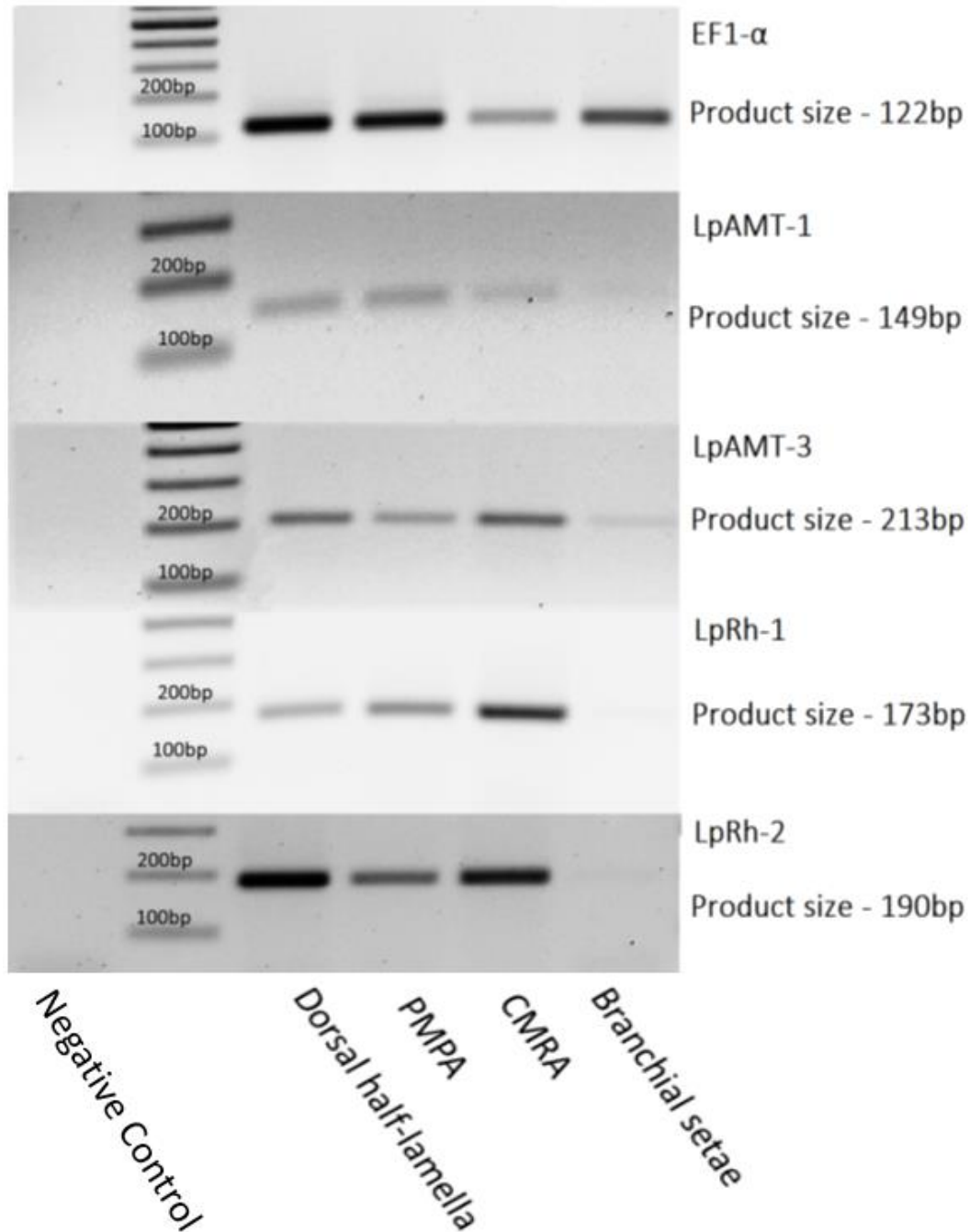


Figure 3: Qualitative PCR results across the four tissue sections. Dorsal half lamellae, peripheral mitochondria poor area (PMPA), central mitochondrial rich area (CMRA), branchial setae. Transcripts and predicted amplicon sizes: elongation factor 1- α (122 bp), LpAMT-1 (149bp) LpAMT-3 (213bp) LpRh-1 (173bp), LpRh-2 (190bp). Visualized on a 1% agarose gel with ethium bromide.

Functional expression of LpAMT1 and LpAMT3

When compared to the sham injected oocytes that had an average $\text{pmol}^{-1} \text{oocyte}^{-1} \text{hour}$ of 122.52 ± 21.05 , all treatment groups had a significant difference in mean (Figure 4). The largest difference was between the coral Rh AyRh which was more than 15x higher than that of sham with a mean of $2024.85 \pm 562.39 \text{ pmol}^{-1} \text{oocyte}^{-1} \text{hour}$ ($p = 3.9^{-15}$). The second positive control, human RhCG was more than 7x higher than the control with a mean of $900.40 \pm 288.76 \text{ pmol}^{-1} \text{oocyte}^{-1} \text{hour}$ ($p=2.8^{-15}$). The two LpAMT groups had means significantly lower than the control. Oocytes injected with LpAMT-1 had a mean cpm 22% lower than the control with a mean of $95.41 \pm 13.99 \text{ pmol}^{-1} \text{oocyte}^{-1} \text{hour}$ ($p=4.15 \times 10^{-7}$). Oocytes injected with LpAMT-3 had a mean cpm of $103.98 \pm 16.00 \text{ pmol}^{-1} \text{oocyte}^{-1} \text{hour}$ which is 15% lower than the control ($p=2.6 \times 10^{-4}$).

Competitive inhibition was measured within treatment groups as opposed to comparing them with the control. In the presence of both 1 mM methylamine and 1 mM of ammonium chloride all treatments showed a significant change in mean uptake, except the sham treatments (Figure 5). No significant difference between the movement of methylamine alone or in the presence of ammonia was detected for the sham treated oocytes at a significance level of $\alpha=0.05$ ($p=0.34$). LpAMT-1 had a significant reduction of 10.8% with a mean of $85.1 \pm 15.11 \text{ pmol}^{-1} \text{oocyte}^{-1} \text{hour}$ ($p=5.7^{-3}$). AyRh had a significant reduction of 14.5% with a mean of $1730.98 \pm 328.411 \text{ pmol}^{-1} \text{oocyte}^{-1} \text{hour}$ ($p= 1.5^{-2}$). Human Rh showed the greatest significant reduction of 36% with a mean of $579.32 \pm 122.67 \text{ pmol}^{-1} \text{oocyte}^{-1} \text{hour}$ ($p= 6.2 \times 10^{-18}$). LpAMT-3 showed a 7% higher mean uptake in the presence of ammonium chloride with a mean value of $111.15 \pm 15.84 \text{ pmol}^{-1} \text{oocyte}^{-1} \text{hour}$ though the test statistic was only just significant ($p=0.049$).

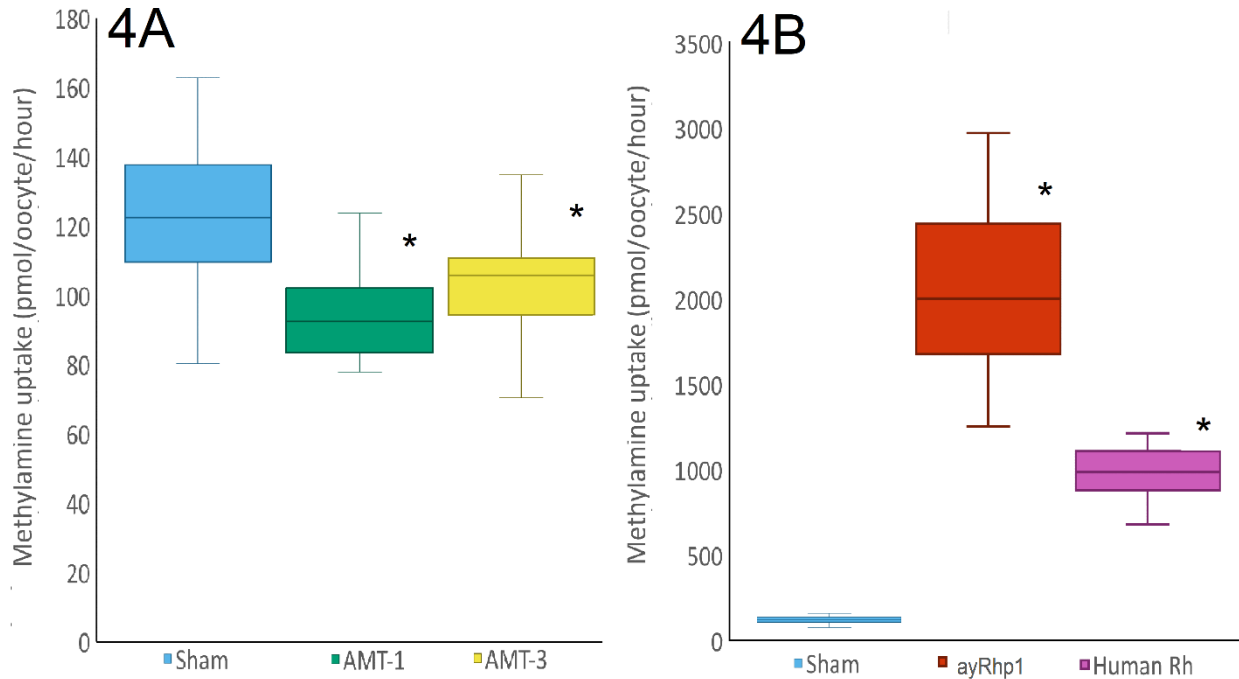


Figure 4: Methylamine uptake in picomole of methylamine per oocyte per hour ($\text{pmol}^{-1} \text{oocyte}^{-1}$ hour) from oocytes injected with the 18 ng cRNA coding for protein LpAMT-1 (4A green, $n=28$), LpAMT-3 (4A yellow, $n=28$), AyRhp-1 (4B red, $n=25$), human Rh (4B purple, $n=27$) molecular grade water (sham, blue, $n=28$). Exposure to 1mM methylamine for 60 minutes with 1 μL of C14 labelled MA per 500 μL . Counts taken for five minutes per oocyte and divided by five to find the average count per minute. Asterisks indicate a mean significantly different than that of sham in an unpaired T= test ($p<0.05$).

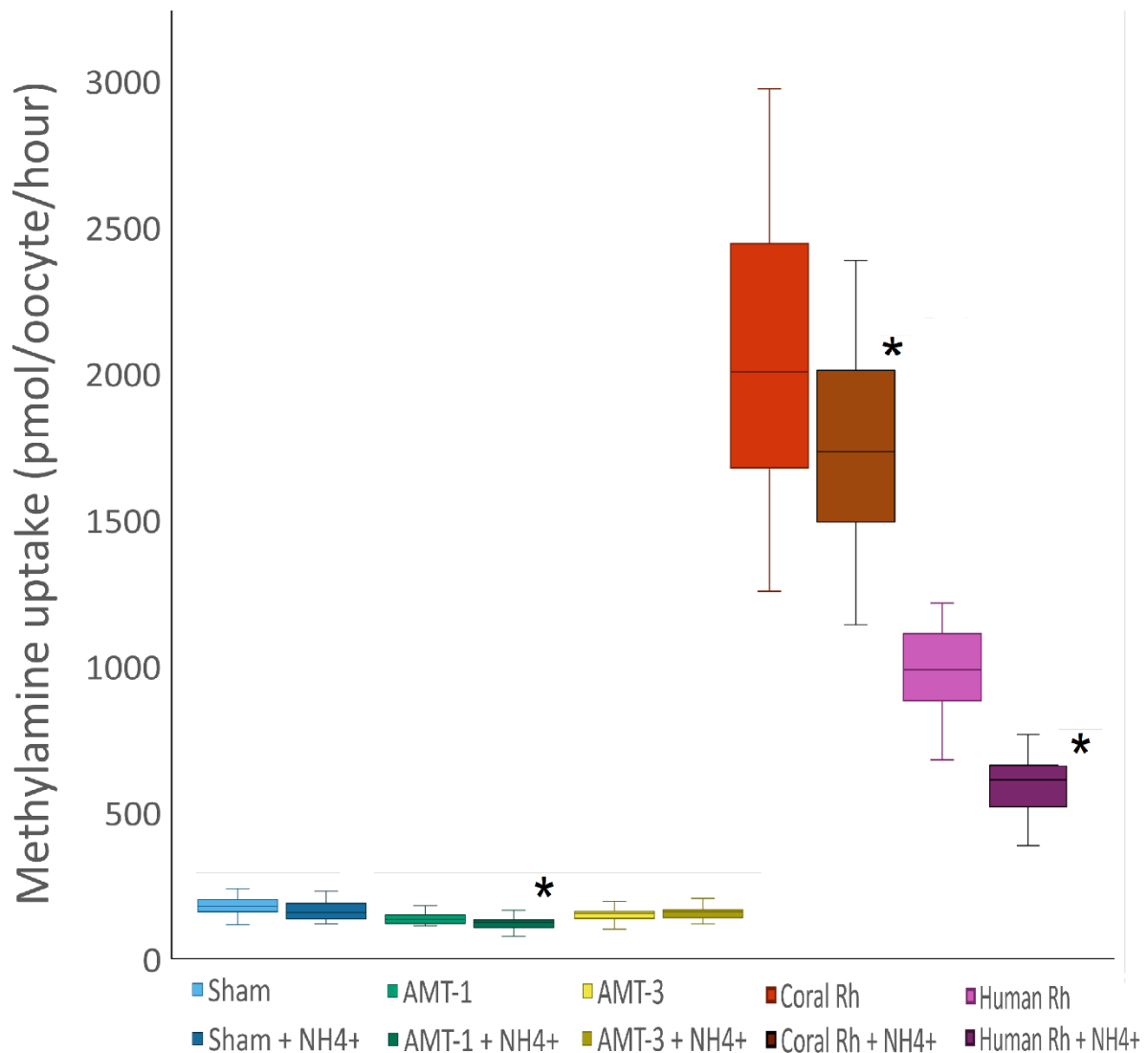


Figure 5: Radiolabelled methylamine uptake in counts per minute per oocyte with competitive inhibition. Exposure to 1 mM methylamine for non inhibition trials and 1 mM methylamine + 1 mM ammonium chloride (+ NH₄⁺) for inhibition trials. Exposure for 60 minutes with 1 μL of C14 labelled MA per 500 μL of incubation buffer. Counts taken for five minutes per oocyte and divided by five to find the average count per minute. Oocytes injected with the 18 ng cRNA coding for proteins LpAMT-1 (green, n=28 non inhibition, n=27 inhibition), LpAMT-3 (yellow, n=28 non inhibition, n=28 inhibition) or molecular grade water (sham, blue, n=28 non inhibition, n=26 inhibition). Asterisks denote a mean significantly different between the methylamine only and methylamine + ammonia groups of the same cRNA insert (p<0.05).

Discussion

Protein alignment

Based on the alignment of LpAMT-1 and LpAMT-3 to the electrogenic AgAMT and the known ammonium transporter AtAmt1:2 an ammonia transport function may be expected (Figure 2). The known highly conserved regions including the twin histidines and the phenylalanine gate are present within all aligned sequences and therefore one would expect the passage of ammonia through the center of each AMT monomer. Regions relevant to the electrogenic function of AtAMT1:2 are also conserved (Neuhäuser and Ludewig 2014), meaning the proton may also be transported through the path between the monomers. However, studies of both bacterial AMT EcAmtB and plant AMT AtAMT1:2 indicate another important region for the transport function within a stretch of amino acids along the C-terminal end that is implicated in the formation of the trimer. Changes to this section on either protein EcAmtB or AtAmt1:2 significantly reduced their transport capability (Severi et al. 2007; Neuhäuser et al. 2007). While it is unknown if changes in this region confers a functional difference without more exploration into both protein structure and function, it is worth noting that all three invertebrate AMTs AgAMT, LpAMT-1 and LpAMT-3 have insertions in this region of between 8 and 14 amino acids of length.

PCR localization

The results of the PCR localization indicates that despite being significantly less permeable to ammonia, the dorsal half lamellae have relatively high expression of transcripts for LpAMT-1, LpAMT-3 and both LpRh proteins. While inferences cannot be made about the degree of expression between the gill regions based on this experiment, the fact that they are all

transcribed to some extent may indicate that they are not being directly used in ammonia excretion, at least within the ammonia impermeable gill sections. The presence of these proteins in the branchial setae leads to further questions about the function of these structures. It is worth noting that while measures were taken to exclude the contamination from genomic DNA it is much more challenging to eliminate entirely the possibility of contamination between gill sections during the splitting procedure. Further quantitative PCR is essential in determining the relative expression of these mRNA sequences across the different tissues.

As both LpAMT-1 and LpAMT-3 are found in the same tissues it is possible that they interact with each other. Hetero-trimerization between more than one type of AtAMT monomer has also been found to reduce transport function (Yuan et al. 2013). Considering that the PCR localization found LpAMT-1 and LpAMT-3 present within all tissue regions it is possible that as in *A. thaliana*, the monomers trimerize in an opportunistic manner and the proportions at which either LpAMT-1 or LpAMT-3 are expressed might be a strategy to regulate protein function and transport rate.

Oocyte expression

Results of the oocyte expression trials suggest that the expression of the *Limulus* AMTs (LpAMT-1 and LpAMT-3) in the *Xenopus* oocytes does not increase the uptake of methylamine into the cell. They may even slightly decrease the uptake of methylamine, though when compared to the 15-fold difference between ayRhp1 and the sham treatments, the difference in mean between AMT-1, AMT-3 and the sham is negligible. Based on the results of the oocyte expression trials, LpAMT-1 and LpAMT-3 there is no evidence they are moving ammonia inward. Whether they are moving ammonia outward or otherwise reducing membrane permeability warrants further exploration.

The functional expression study evaluated the potential ammonia transport function of LpAMT-1 and LpAMT-3 using the analogous substrate ^{14}C -methylamine. A lack of transport might be explained if methylamine was an inappropriate substrate for LpAMT-1 and LpAMT-3. Though methylamine is widely used as an analog for ammonia it is known that for the AMTs of plants there is a significant difference in substrate affinity between ammonia and methylamine. For example, tissue wide assimilation of nitrogen in the roots of tomato plants is tenfold higher when using ammonia as a substrate compared to methylamine, and methylamine is not considered to be an appropriate analogue unless there is little to no presence of surrounding ammonia (Kosola and Bloom 1994). Methylamine is not ammonia and it was shown that in Rh proteins the responses are different when measuring ammonia compared to methylamine transport (Nakhoul and Lee Hamm 2014). Further experiments should be run using ammonia itself in order to exclude this possibility. There is also the possibility that LpAMT-1 and LpAMT-3 were not translated into functional proteins in the *Xenopus* oocyte, or that the protein was correctly translated/folded but not integrated into the oocyte membrane. Future experiments should include some direct protein measurement and localization to ensure that the mRNA is being translated and that the protein is being incorporated into the oocyte membrane. This could involve antibody localization and Western blot analyses. Both positive Rh controls showed significantly higher transport properties than all other treatments, illustrating that my oocytes were in good condition and protocols were appropriate for their expression and integration into the membrane.

There is also evidence that plant-like AMTs are pH dependent (Wacker et al. 2014) which may be a factor in my results as the experiments were run at a single pH (7.5). However, the pH within the tissues of animals is highly controlled and rarely variable while plants,

particularly in regions that are taking in nitrogen (the roots), have acidified cell walls to facilitate cell elongation (Barbez et al. 2017). It is unlikely that an invertebrate animal in the highly buffered seawater environment would be exposed to pH levels beyond a narrow physiological range in the way that plant tissues might be. Many plants tolerate extracellular pH as low as 4, while horseshoe crabs exposed to air for short periods to induce hypoxia stress had hemolymph pH levels comparable to my trials (between 7.1 and 7.3) and extreme hypoxia stress for 24 hours did not alter hemolymph concentrations lower than 6.68 (Allender et al. 2010). Therefore, even if large changes in pH alter transport ability, it would likely not be representative of the proteins function in animal tissue.

It is possible that while LpAMT-1 and LpAMT-3 are not transporting methylamine, they are instead transporting the dissociated proton. Previous studies with *A. thaliana* have functionally uncoupled the two transport functions which indicates that the functions are not necessarily paired or dependent upon each other. Previous studies on invertebrate AMT AgAMT demonstrated a significant increase in inward currents in oocytes expressing the protein, though did not however show evidence of ammonia movement, as transformed MEP deficient yeast strains failed to culture on media with ammonia as its sole nitrogen source (Pitts et al. 2014). It is possible that the transport of ammonia through the pore of each monomer is disrupted while maintaining the proton transport between the monomers. Functionally, this would result in a channel for protons with an extracellular ammonia deprotonation region. If this were the case the reduction of methylamine transport in the LpAMT-1 and LpAMT-3 treatment groups might be explained by an influx of protons reducing the oocytes overall electronegativity or by a cell wide response to changes in cytoplasmic pH levels. This warrants further exploration into the ion specific electrogenic activity of this class of proteins.

Conclusion

Few concrete conclusions can be made other than the need for more data. There is however little evidence to support the conclusion that invertebrate AMT proteins are involved in the direct bulk excretion of ammonia in the way that it has been suggested. There is a lack in functional expression studies overall and the studies that are done in the future must be more intensive to determine if ammonia transport is occurring. Future research should involve a combination of both nitrogen assimilation and electrogenic measurements to determine if NH_4^+ is the molecule involved. This may include both yeast complementation assays to confirm the movement of nitrogen and the Selective Ion Electrode Technique to determine which ion is passing over the membrane. Additional oocyte expression studies should include direct measurement of ammonia as a substrate in order to eliminate the possibility that they are simply poor methylamine transporters. It would also be advised to measure the proteins directly, both for abundance and for their integration into the membrane.

Literature

- Adlimoghaddam, A., Boeckstaens, M., Marini, A.-M., Treberg, J.R., Brassinga, A.-K.C., and Weihrauch, D. 2015. Ammonia excretion in *Caenorhabditis elegans*: mechanism and evidence of ammonia transport of the Rhesus protein CeRhr-1. *J. Exp. Biol.* **218**(5): 675–683. doi:10.1242/jeb.111856.
- Allender, M., Schumacher, J., George, R., Milam, J., and Odoi, A. 2010. The effects of short- and long-term hypoxia on hemolymph gas values in the American horseshoe crab (*Limulus polyphemus*) using a point-of-care analyzer. *J. Zoo Wildl. Med. Off. Publ. Am. Assoc. Zoo Vet.* **41**: 193–200. doi:10.1638/2008-0175R2.1.
- Andrade, S.L.A., and Einsle, O. 2007. The Amt/Mep/Rh family of ammonium transport proteins (Review). *Mol. Membr. Biol.* **24**(5–6): 357–365. Taylor & Francis. doi:10.1080/09687680701388423.
- Ballesteros, J.A., and Sharma, P.P. 2019. A critical appraisal of the placement of *Xiphosura* (Chelicerata) with account of known sources of phylogenetic error. *Syst. Biol.* **68**(6): 896–917. doi:10.1093/sysbio/syz011.
- Barbez, E., Dünser, K., Gaidora, A., Lendl, T., and Busch, W. 2017. Auxin steers root cell expansion via apoplastic pH regulation in *Arabidopsis thaliana*. *Proc. Natl. Acad. Sci.* **114**(24): E4884–E4893. Proceedings of the National Academy of Sciences. doi:10.1073/pnas.1613499114.
- Binstock, L., and Lecar, H. 1969. Ammonium ion currents in the squid giant axon. *J. Gen. Physiol.* **53**(3): 342–361. doi:10.1085/jgp.53.3.342.
- Biswas, K., and Morschhäuser, J. 2005. The Mep2p ammonium permease controls nitrogen starvation-induced filamentous growth in *Candida albicans*. *Mol. Microbiol.* **56**(3): 649–669. doi:10.1111/j.1365-2958.2005.04576.x.
- Chasiotis, H., Ionescu, A., Misyura, L., Bui, P., Fazio, K., Wang, J., Patrick, M., Weihrauch, D., and Donini, A. 2016. An animal homolog of plant Mep/Amt transporters promotes ammonia excretion by the anal papillae of the disease vector mosquito *Aedes aegypti*. *J. Exp. Biol.* **219**(9): 1346–1355. doi:10.1242/jeb.134494.
- Durant, A.C., and Donini, A. 2018. Ammonia excretion in an osmoregulatory syncytium is facilitated by AeAmt2, a novel ammonia transporter in *Aedes aegypti* larvae. *Front. Physiol.* **9**. Available from <https://www.frontiersin.org/article/10.3389/fphys.2018.00339> [accessed 19 May 2022].
- Goldin, A.L. 1993. *Xenopus* oocytes as an expression system for ion channels. In *Methods in Pharmacology: Molecular and Cellular Biology of Pharmacological Targets*. Edited by H. Glossmann and J. Striessnig. Springer US, Boston, MA. pp. 79–97. doi:10.1007/978-1-4757-2239-0_4.
- Hans, S., Quijada-Rodriguez, A.R., Allen, G.J.P., Onken, H., Treberg, J.R., and Weihrauch, D. 2018. Ammonia excretion and acid–base regulation in the American horseshoe crab, *Limulus polyphemus*. *J. Exp. Biol.* **221**(6): jeb151894. doi:10.1242/jeb.151894.
- Howitt, S.M., and Udvardi, M.K. 2000. Structure, function and regulation of ammonium transporters in plants. *Biochim. Biophys. Acta BBA - Biomembr.* **1465**(1): 152–170. doi:10.1016/S0005-2736(00)00136-X.
- Huang, C.-H., and Peng, J. 2005. Evolutionary conservation and diversification of Rh family genes and proteins. *Proc. Natl. Acad. Sci.* **102**(43): 15512–15517. doi:10.1073/pnas.0507886102.
- Javelle, A., Lupo, D., Zheng, L., Li, X.-D., Winkler, F.K., and Merrick, M. 2006. An unusual twin-His arrangement in the pore of ammonia channels is essential for substrate conductance. *J. Biol. Chem.* **281**(51): 39492–39498. doi:10.1074/jbc.M608325200.
- Kosola, K.R., and Bloom, A.J. 1994. Methylammonium as a transport analog for ammonium in tomato (*Lycopersicon esculentum* L.). *Plant Physiol.* **105**(1): 435–442. American Society of Plant Biologists (ASPB).

- Lamsdell, J.C. 2020. The phylogeny and systematics of *Xiphosura*. PeerJ **8**: e10431. doi:10.7717/peerj.10431.
- Larsen, E.H., Deaton, L.E., Onken, H., O'Donnell, M., Grosell, M., Dantzler, W.H., and Weihrauch, D. 2014. Osmoregulation and excretion. In *Comprehensive Physiology*. John Wiley & Sons, Ltd. pp. 405–573. doi:10.1002/cphy.c130004.
- Lorenz, M.C., and Heitman, J. 1998. The MEP2 ammonium permease regulates pseudohyphal differentiation in *Saccharomyces cerevisiae*. EMBO J. **17**(5): 1236–1247. John Wiley & Sons, Ltd. doi:10.1093/emboj/17.5.1236.
- Marini, A.-M., Matassi, G., Raynal, V., André, B., Cartron, J.-P., and Chérif-Zahar, B. 2000. The human Rhesus-associated RhAG protein and a kidney homologue promote ammonium transport in yeast. Nat. Genet. **26**(3): 341–344. Nature Publishing Group. doi:10.1038/81656.
- McDonald, T.R., and Ward, J.M. 2016. Evolution of electrogenic ammonium transporters (AMTs). Front. Plant Sci. **7**. Available from <https://www.frontiersin.org/articles/10.3389/fpls.2016.00352> [accessed 20 August 2022].
- Miller, A.J., and Zhou, J.J. 2000. *Xenopus* oocytes as an expression system for plant transporters. Biochim. Biophys. Acta BBA - Biomembr. **1465**(1): 343–358. doi:10.1016/S0005-2736(00)00148-6.
- Molnár, R.L., and Fekete, V.A. 2011. Ammonia: structure, biosynthesis, and functions. Nova Science Publishers, Inc, Hauppauge, N.Y. Available from <http://uml.idm.oclc.org/login?url=https://search.ebscohost.com/login.aspx?direct=true&db=e000xna&AN=541726&site=ehost-live> [accessed 24 November 2022].
- Nakhoul, N.L., and Lee Hamm, L. 2014. The challenge of determining the role of Rh glycoproteins in transport of NH₃ and NH₄⁺. Wiley Interdiscip. Rev. Membr. Transp. Signal. **3**(3): 53–61. doi:10.1002/wmts.105.
- Neuhäuser, B., Dynowski, M., Mayer, M., and Ludewig, U. 2007. Regulation of NH₄⁺ transport by essential cross talk between AMT monomers through the carboxyl tails. Plant Physiol. **143**(4): 1651–1659. doi:10.1104/pp.106.094243.
- Neuhäuser, B., and Ludewig, U. 2014. Uncoupling of ionic currents from substrate transport in the plant ammonium transporter AtAMT1;2. J. Biol. Chem. **289**(17): 11650–11655. doi:10.1074/jbc.C114.552802.
- Ninnemann, O., Jauniaux, J.C., and Frommer, W.B. 1994. Identification of a high affinity NH₄⁺ transporter from plants. EMBO J. **13**(15): 3464–3471.
- Peng, J., and Huang, C.H. 2006. Rh proteins vs Amt proteins: an organismal and phylogenetic perspective on CO₂ and NH₃ gas channels. Transfus. Clin. Biol. **13**(1): 85–94. doi:10.1016/j.tracli.2006.02.006.
- Pitts, R.J., Derryberry, S.L., Pulous, F.E., and Zwiebel, L.J. 2014. Antennal-expressed ammonium transporters in the malaria vector mosquito *Anopheles gambiae*. PLoS ONE **9**(10): e111858. doi:10.1371/journal.pone.0111858.
- Severi, E., Javelle, A., and Merrick, M. 2007. The conserved carboxy-terminal region of the ammonia channel AmtB plays a critical role in channel function. Mol. Membr. Biol. **24**(2): 161–171. Taylor & Francis. doi:10.1080/09687860601129420.
- Thiel, D., Hugenschütt, M., Meyer, H., Paululat, A., Quijada-Rodriguez, A.R., Purschke, G., and Weihrauch, D. 2017. Ammonia excretion in the marine polychaete *Eurythoe complanata* (Annelida). J. Exp. Biol. **220**(3): 425–436. doi:10.1242/jeb.145615.
- Thies, A.B., Quijada-Rodriguez, A.R., Zhouyao, H., Weihrauch, D., and Tresguerres, M. 2022. A Rhesus channel in the coral symbiosome membrane suggests a novel mechanism to regulate NH₃ and CO₂ delivery to algal symbionts. Sci. Adv. **8**(10): eabm0303. American Association for the Advancement of Science. doi:10.1126/sciadv.abm0303.

- Tremblay, P.-L., and Hallenbeck, P.C. 2009. Of blood, brains and bacteria, the Amt/Rh transporter family: emerging role of Amt as a unique microbial sensor. *Mol. Microbiol.* **71**(1): 12–22. doi:10.1111/j.1365-2958.2008.06514.x.
- Vulpe, A., Kim, H.S., Ballou, S., Wu, S.-T., Grabe, V., Nava Gonzales, C., Liang, T., Sachse, S., Jeanne, J.M., Su, C.-Y., and Menuz, K. 2021. An ammonium transporter is a non-canonical olfactory receptor for ammonia. *Curr. Biol. CB* **31**(15): 3382-3390.e7. doi:10.1016/j.cub.2021.05.025.
- Wacker, T., Garcia-Celma, J.J., Lewe, P., and Andrade, S.L.A. 2014. Direct observation of electrogenic NH₄⁺ transport in ammonium transport (Amt) proteins. *Proc. Natl. Acad. Sci.* **111**(27): 9995–10000. *Proceedings of the National Academy of Sciences.* doi:10.1073/pnas.1406409111.
- Wright, J., O'Donnell, M., and Reichert, J. 1994. Effects of ammonia loading on *Porcellio scaber*: Glutamine and glutamate synthesis, ammonia excretion and toxicity. *J. Exp. Biol.* **188**: 143–57. doi:10.1242/jeb.188.1.143.
- Wright, P.A. 1995. Nitrogen excretion: three end products, many physiological roles. *J. Exp. Biol.* **198**(2): 273–281. doi:10.1242/jeb.198.2.273.
- Yuan, L., Gu, R., Xuan, Y., Smith-Valle, E., Loqué, D., Frommer, W.B., and von Wirén, N. 2013. Allosteric regulation of transport activity by heterotrimerization of *Arabidopsis* ammonium transporter complexes in vivo. *Plant Cell* **25**(3): 974–984. doi:10.1105/tpc.112.108027.